Journal of Nuclear and Particle Physics 2013, 3(4): 108-120
DOI: 10.5923/j.jnpp.20130304.08

Cross Sections for the Astrophysical Neutron Radiative Capture on ^{12}C and ^{13}C Nuclei

S. B. Dubovichenko[1,*], A. V. Dzhazairov-Kakhramanov[2], N. A. Burkova[3]

[1]V.G. Fessenkov Astrophysical Institute "NCSRT" NSA RK, 050020, Almaty, Kazakhstan
[2]Institute of Nuclear physics RK, 050032, str. Ibragimova 1, Almaty, Kazakhstan
[3]Al-Farabi Kazakh National University, 050040, av. Al-Farabi 71, Almaty, Kazakhstan

Abstract We continue to study the radiative capture processes on light nuclei, and are treating here neutron capture reactions on ^{12}C and ^{13}C at astrophysical energies, that included in one of the variants of reaction chains for inhomogeneous Big Bang models. Within the potential cluster model with Pauli forbidden states the possibility of description of the experimental data on the total radiative n^{12}C and n^{13}C capture cross sections in the astrophysical energy range from 25 meV to 1.0 MeV is presented. The *E*1 transition covers the capture data from the scattering states to the ground one of ^{13}C and ^{14}C nuclei. Capture on the three low laying excited states $1/2^+$, $3/2^-$ and $5/2^+$ of ^{13}C was calculated. Also we have considered the radiative neutron capture on ^{13}C for transitions to the GS and to the first ES of ^{14}C are in a wonderful agreement with the new experimental data[A. Wallner *et al*., 2012], which became known for us after finishing these calculations.

Keywords Neutron Radiative Capture Cross Sections, Potential Cluster Model, Pauli Forbidden States, Young Tableaux, Phase Shifts, Nuclear Astrophysics, Primordial Nucleosynthesis, Inhomogeneous Big Bang Models

1. Introduction

Our last works[1-3] reported the data on the astrophysical *S*-factors[4, 5] for 10 radiative capture reactions on light nuclei treated on the basis of the potential cluster model (PCM) with Pauli forbidden states (FS). Classification of the cluster orbital states in the PCM make it possible to define the existence and number of the allowed states (AS) in two-body potentials[6]. The results of the phase shift analysis of the experimental data on the differential cross sections of elastic scattering of corresponding free nuclei are used for the construction of phenomenological two-body interaction potentials for the scattering states in the PCM[7-9].

Potentials for the bound states (BS) of light nuclei in cluster channels are constructed not only on the basis of phase shifts, but also under some additional demands. So, they should reproduce the binding energy in corresponding nuclear system as well as some other characteristics of nuclei[1-3]. The choice of the PCM for treating of cluster systems and thermonuclear processes at astrophysical energies[4, 10] is caused by the fact, that in lots of atomic nuclei the probability of forming of the nucleon associations (clusters), and the degree of their isolation from each other are comparatively high. This is confirmed by the numerous experimental data and different theoretical calculations implemented over the past fifty years[1, 6, 9, 11, 12].

We continue to study the radiative capture processes on light nuclei, and are treating here neutron capture reactions on ^{12}C and ^{13}C at astrophysical energies, that included in one of the variants of reaction chains for inhomogeneous Big Bang models[13-17].

$$^1\mathrm{H}(n,\gamma)^2\mathrm{H}(n,\gamma)^3\mathrm{H}(^2\mathrm{H},n)^4\mathrm{He}(^3\mathrm{H},\gamma)^7\mathrm{Li}(n,\gamma)^8\mathrm{Li}(^4\mathrm{He},n)$$
$$^{11}\mathrm{B}(n,\gamma)^{12}\mathrm{B}(\beta^-)\underline{^{12}\mathrm{C}(n,\gamma)^{13}\mathrm{C}(n,\gamma)^{14}\mathrm{C}}(p,\gamma)^{15}\mathrm{N}(n,\gamma)^{16}\mathrm{N}\ldots . \quad (1)$$

Apparently these very reactions led finally to the formation of the Sun, stars and our Universe[1, 14]. Available experimental data on the total cross sections, for example, for the ^{12}C(*n*, γ)^{13}C reaction are given in[18-24] and may be found also in data bases[25, 26]. Since, they do not cover the total energy scale for the processes of the Universe formation, but give the common representation on the behavior of radiative capture cross sections in wide energy range.

The ^{13}C(*n*, γ)^{14}C reaction acts as neutron poison in *s*-process nucleosynthesis. Moreover, via this neutron capture reaction, another ingredient for *s*-process nucleosynthesis is removed: the primary ^{13}C nuclide, which forms the target for the neutron production via ^{13}C(α, n), is transformed to ^{14}C. That is why, it is actual to describe these cross sections within the PCM with FS as it was done for the proton radiative capture on ^{12}C and ^{13}C[27, 28].

Note, recently done phase shifts analysis of new experimental data on the p^{12}C and p^{13}C scattering at

* Corresponding author:
dubovichenko@mail.ru (S. B. Dubovichenko)
Published online at http://journal.sapub.org/jnpp

astrophysical energies[29, 30] made it possible to construct quite unambiguous $p^{13}C$ and $p^{12}C$ potentials. They should not differ essentially from the analogue potentials for the $n^{12}C$ and $n^{13}C$ scattering and bound states of ^{13}C in the $n^{12}C$ channel and ^{14}C in the $n^{13}C$ channel. Furthermore, we are following the standpoint that the $p^{12}C$ and $n^{12}C$ channels (as well as the $p^{12}C$ and $n^{12}C$ systems) are the isobar analogues. Actually it is reasonable to examine them in comparative way.

2. Model and Methods

Classification of orbital states for the $n^{12}C$ and $p^{12}C$ systems by Young tableaux was treated in work[27]. It was shown that complete system of 13 nucleons may have the set of Young tableaux {1} × {444} = {544} + {4441}. The first of the obtained tableau is compatible with the orbital momentum L = 0 only and is forbidden, so far as it could not be five nucleons in the *s*-shell.

The second tableau is allowed and compatible with the angular moments L = 1 and 3 defined according the Elliot' rules[31]. State with L = 1 corresponds to the ground bound allowed state of ^{13}C in the $n^{12}C$ channel with quantum numbers J^{π},T = 1/2$^-$,1/2. So, there might be one forbidden bound state in ^2S wave potential, and ^2P wave should have the allowed state only in the $n^{12}C$ channel at the energy -4.94635 MeV[32].

Classification of orbital states for the $p^{13}C$ system, and hence $n^{13}C$ one by the Young tableaux we did in[28]. So, let us remind shortly that for the $p^{13}C$ system within the 1*p*-shell we got {1} × {4441} → {5441} + {4442}[28]. The first of the obtained tableau is compatible with the orbital moment L = 1 only. It is forbidden as five nucleons can not occupy the *s*-shell. The second tableau is allowed and is compatible with the angular moments L = 0 and 2[31]. Thus, restricting by the lowest partial waves we conclude that there is no forbidden state in the $^3S_1$ potential, but the ^3P wave has both one forbidden and one allowed states. The last one appeared at the binding energy -8.1765 MeV of the $n^{13}C$ system and corresponds the ground state of ^{14}C in this channel with J^{π} = 0^+[32].

However, we regard the results on the classification of ^{13}C and ^{14}C nuclei by orbital symmetry in $n^{12}C$ and $n^{13}C$ channels as the qualitative ones as there are no complete tables of Young tableaux productions for the systems with a number of nucleons more than eight[32], which have been used in earlier similar calculations[2, 34, 35]. At the same time, just on the basis of such classification we succeeded with description of available experimental data on the proton radiative capture on ^{12}C and ^{13}C[27, 28]. That is why the given above classification procedure by orbital symmetry was used for the determination of a number of forbidden and allowed states in two-body potentials. Note, as the isospin projection in the $n^{13}C$ system T_z = -1, then the total isospin T = 1, and this is the first cluster system among all treated earlier ones pure by isospin with its maximum value[1-3].

The potential in the Gaussian form as usual in[1-3] with a point-like Coulomb term is using for the two-body interaction

$$V(r) = -V_0 \exp(-\alpha r^2). \quad (2)$$

For the calculation of nuclear characteristics additional control on the computing of ^{13}C and ^{14}C binding energy in ground state along with the finite-difference method (FDM) – the variational method (VM) was used. In the variational method, the expansion of cluster relative motion wave function (WF) by non-orthogonal Gaussian basis was used, and independent parameter variation was performed[3, 36]. The wave function itself has the form[22]

$$\Phi_{\mathrm{L}}(r) = \frac{\chi_{\mathrm{L}}(R)}{r} = Nr^{\mathrm{L}} \sum_{\mathrm{i}} C_{\mathrm{i}} \exp(-\beta_{\mathrm{i}} r^2), \quad (3)$$

where β_i are the variational parameters and C_i are the expansion coefficients, N is the normalization coefficient of WF.

The behavior of wave functions for bound states (BS) at large distances was controlled by the asymptotic constant (AC) C_W determining by the Whittaker function of the form[37, 38]

$$\chi_L(r) = \sqrt{2k}_0 C_{\mathrm{W}} W_{-\eta L+1/2}(2kr). \quad (4)$$

Here $\chi_L(r)$ is the numerical wave function of the bound state obtained from the solution of the radial Schrödinger equation and normalized to unity; $W_{-\eta L+1/2}$ is the Whittaker function of the bound state determining the asymptotic behavior of the wave function which is the solution to the same equation without the nuclear potential; i.e., at large distances; k is the wave number determined by the channel binding energy; η is the Coulomb parameter; and L is the angular momentum of the bound state.

Total radiative cross sections $\sigma(EJ)$ in case of potential cluster model have the following form – see, for example,[39] or[40]:

$$\sigma_C(EJ, J_{\mathrm{f}}) = \frac{8\pi K e^2}{\hbar^2 q^3} \frac{\mu}{(2S_1+1)(2S_2+1)} \frac{J+1}{J[(2J+1)!!]^2} \times A_{\mathrm{J}}^2(K) \sum_{\mathrm{L_i,J_i}} |P_{\mathrm{J}}(EJ, J_{\mathrm{f}}, J_{\mathrm{i}}) I_{\mathrm{J}}(J_{\mathrm{f}}, J_{\mathrm{i}})|^2, \quad (5)$$

where for convective electric $EJ(L)$ transitions well known expressions are used[39-41]

$$P_{\mathrm{J}}^2(EJ, J_{\mathrm{f}}, J_{\mathrm{i}}) = \delta_{\mathrm{S_i S_f}} \left[(2J+1)(2L_{\mathrm{i}}+1)(2J_{\mathrm{i}}+1)(2J_{\mathrm{f}}+1)\right](L_{\mathrm{i}}0J0 \mid L_{\mathrm{f}}0)^2 \begin{Bmatrix} L_{\mathrm{i}} & S & J_{\mathrm{i}} \\ J_{\mathrm{f}} & J & L_{\mathrm{f}} \end{Bmatrix}^2, \quad (6)$$

$$A_{\mathrm{J}}(K) = K^{\mathrm{J}} \mu^{\mathrm{J}} \left[\frac{Z_1}{m^{\mathrm{J}}{}_1} + (-1)^{\mathrm{J}} \frac{Z_2}{m^{\mathrm{J}}{}_2} \right], \quad I_{\mathrm{J}}(J_{\mathrm{f}}, J_{\mathrm{i}}) = \left\langle L_{\mathrm{f}} J_{\mathrm{f}} \left| R^{\mathrm{J}} \right| L_{\mathrm{i}} J_{\mathrm{i}} \right\rangle. \quad (7)$$

Here μ – reduced mass of colliding particles; q – wave number in initial channel; L_i, L_f, J_i, J_f –angular and total moments in initial (i) and final (f) channels; S_1, S_2 – particles spins in initial channel; m_1, m_2, Z_1, Z_2 – masses and charges of particles in initial channel; S_i, S_f – total spins in initial and final channels (here $S_i = S_f = S$); K, J – wave number and momentum of γ-quantum; I_J – overlapping integral of cluster WF and corresponding radial part of $EJ(L)$-transition operator. Let us note, that in our present calculations as well as in previous we nether used such a characteristic as spectroscopic factor - see for example[39], i. e., its value is assumed unit.

We used in our calculations the exact values for particle masses m_n = 1.00866491597[42], $m_{^{13}C}$ = 13.00335502 amu[43], constant $\hbar^2/m_0$ was assumed 41.4686 MeV fm^2. For proton capture point like Coulomb potential was used in the form V_{Coul}(MeV) = 1.439975 Z_1 Z_2/r, where r – relative distance between the particles in initial channel in fermi (fm), Z – charges of particles in elementary charge units. Coulomb parameter $\eta = \mu Z_1 Z_2 e^2/(k\hbar^2)$ was used in the form η = 3.44476 10^{-2} Z_1 Z_2 μ/k, here wave number k in fm^{-1} is defined by the energy E of interacting particles $k^2 = 2\mu E/\hbar^2$.

3. Total Cross Sections for Neutron Capture on ^{12}C

Firstly note that the processes of the neutron capture by ^{12}C on the GS and three ES were considered, for example in the model of direct capture[44-46], where the good description of the existent experimental data in the energy range from 20 to 200 KeV was obtained. The dependence of total cross section of the n^{12}C capture for transitions from different partial scattering wave was shown in[19] on the basis of direct capture model too. In addition, the possibility to describe the neutron capture on ^{12}C in the energy range from 20 to 600 KeV was studied in[47] on the basis of generalized optic model. Also, there is one interesting work devoted to cross section expansion for direct neutron radiative capture in the energy range from 20 to 600 KeV[48]. Simultaneously note that we have not found any works where this reaction was considered in so wide energy range (from 25 meV to 1.0 MeV), as we are studying it in this paper.

Here we are following the declared concept that the p^{12}C and n^{12}C channels are the isobar analogues. So, we are doing their analysis in comparison. Early in works[27] and[29] the interaction potential for the $^2S_{1/2}$ wave in the p^{12}C scattering channel was constructed in a way to describe correctly the corresponding partial elastic scattering phase shift which has the pronounced resonance at 0.42 MeV.

On the contrary, in the n^{12}C system there are no resonances according[32] up to 1.9 MeV. So, in this channel the $^2S_{1/2}$ phase shift should reveal smooth behavior in this energy region. We were unable to find in the literature the results of phase analysis for the n^{12}C elastic scattering at the energies below 1.0-1.5 MeV[25, 26], and we suppose they should differ notably from those in the p^{12}C scattering channel[30]. That is why for determine of the proper behavior of ^2S phase shift the corresponding phase analysis of the n^{12}C elastic scattering was done at astrophysical energies, viz. from 50 KeV to 1.0 MeV[49]. Experimental measurements of differential elastic scattering cross sections in the energy range from 0.05 up to 2.3 MeV was done in[50]. Results of our analysis for the ^2S phase shift are presented in Fig. 1a by black dots.

In present calculations of the radiative neutron capture on ^{12}C, the dipole electric $E1(L)$ transition corresponding to the convective part of $Q_{JM}(L)$ operator[27, 29] was taken into account. This transition in n^{12}C $\rightarrow$ ^{13}Cγ process occurs from the $^2S_{1/2}$ doublet scattering state onto $^2P_{1/2}$ ground state of ^{13}C bound in the n^{12}C channel, i.e., the reaction of ^{12}C(n, γ_0)^{13}C type is treated. Evaluation of $E1$-transion from ^2D scattering state to the ground state (GS) shows the cross section two-three orders magnitude less.

Firstly, a potential for the GS of ^{13}C in the n^{12}C channel without FS was constructed following the results obtained earlier for the p^{12}C system[27]. It should reproduce the binding energy of the ground $^2P_{1/2}$ state of ^{13}C in the n^{12}C channel equals -4.94635 MeV, as well as value of mean square radius 2.4628(39) fm[32]. The radius of ^{12}C of 2.4702(22) fm was taken from[43] comparing 2.4829(19) fm[51]; neutron charge radius is zero, and its mass radius is taken as proton one 0.8775(51) fm[42]. So, the following central potential was obtained for the p^{12}C system and n^{12}C channel:

$$V_{GS} = 135.685685 \text{ MeV}, \ \alpha_{GS} = 0.425 \text{ fm}^{-2}. \quad (8)$$

Potential (8) gives the binding energy of -4.946350 MeV with accuracy of 10^{-6} by FDM, mean square charge radius of R_{ch} = 2.48 fm, and mass radius of R_m = 2.46 fm. Asymptotic constant turned equals 0.99(1) on the interval of 5-13 fm. Error for the AC is defined by averaging over the pointed interval.

Let us note, that according data[51] and[52], where the compilation of many results is presented, the obtained value for this constant recalculated with $\sqrt{2k} = 0.971$ to the dimensionless quantity is 1.59(3). According data[17] this value after recalculation is 1.99(18). The redefinition is coming due to another specification for AC differing from our by factor $\sqrt{2k}$

$$\chi_L(R) = C_W W_{-\eta L+1/2}(2kR). \quad (9)$$

There is another set of parameters for n^{12}C potential reproducing the GS of ^{13}C

$$V_{GS} = 72.173484 \text{ MeV}, \ \alpha_{GS} = 0.2 \text{ fm}^{-2}. \quad (10)$$

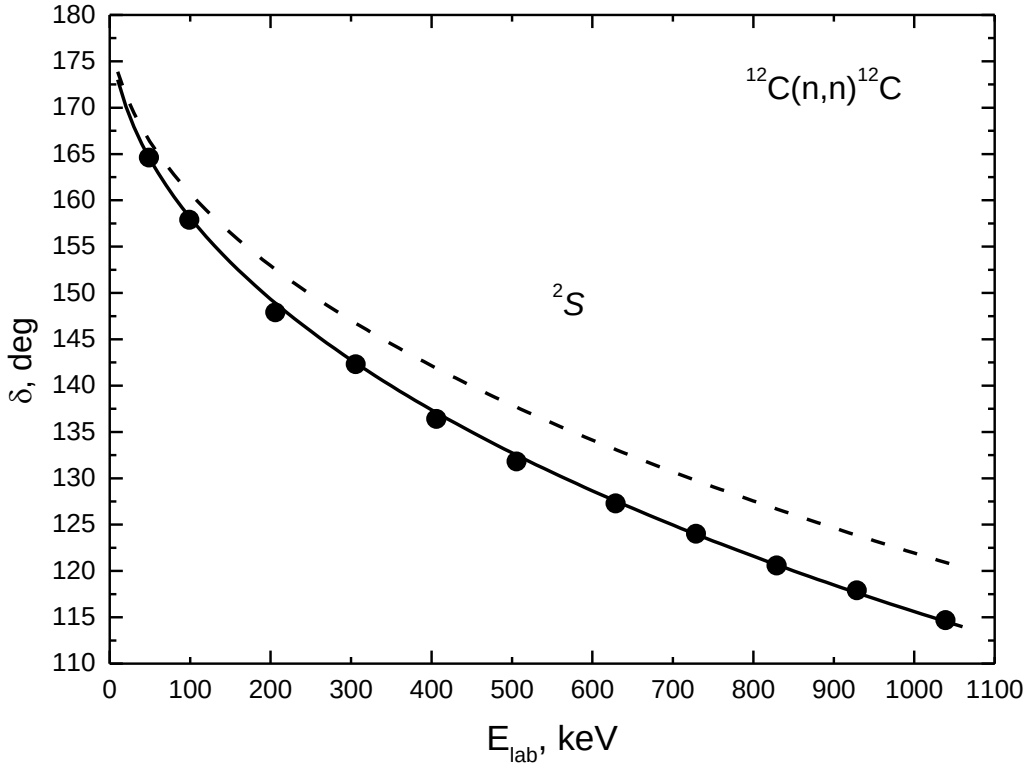

Figure 1a. Low energy $^2S_{1/2}$-phase shift of elastic n^{12}C-scattering. Results of our ^2S phase shift analysis – black dots (●) –[49]. Calculations with potential given in text according to (12)

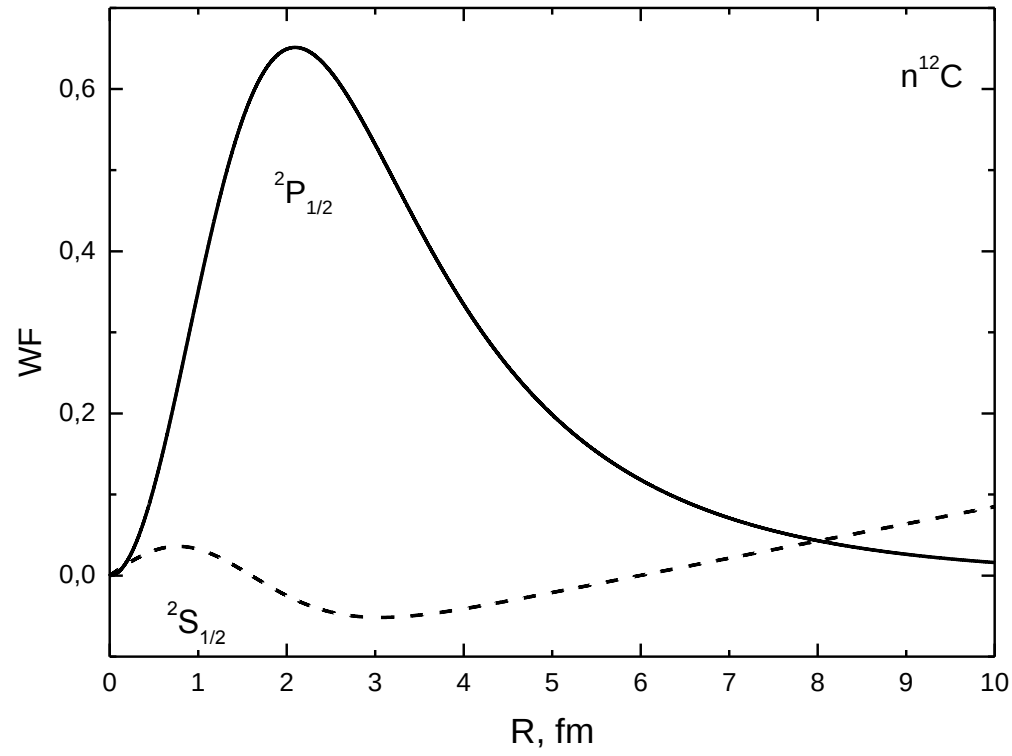

Figure 1b. Radial wave functions of the $^2P_{1/2}$ ground state of ^{13}C in the n^{12}C channel and the $^2S_{1/2}$ scattering wave at 10 KeV

This potential leads to the binding energy of -4.94635034 MeV with accuracy of 10^{-8} by the FDM and same charge radius of 2.48 fm, but mean square mass radius equals R_m = 2.51 fm is a little bit greater, and AC equals 1.52(1) within the interval of 5-18 fm agrees better with data[17, 52, 53]. Solid line in Fig. 1b shows the WF of such $^2P_{1/2}$ potential.

As the additional computing control for the calculation of binding energy with potential (10) variational method was

applied[36]. It gave the energy value of -4.94635032 MeV with dimension $N = 10$ and independent parameter' varying of potential (10). Asymptotic constant C_W of the variational WF is 1.52(2) within the interval of 5-15 fm while the residual does not exceed 10^{-12}[3]. Charge radius is the same as obtained by FDM. The variational energy decreases at the increasing of basis dimension and reaches the upper limit of true binding energy, and the finite-differential energy increases at the reducing of step value and increasing of step number, then it is reasonable to assume the average value for the binding energy of -4.94635033(1) MeV as valid. The accuracy of both methods is equal to ± 10 meV.

Following the declared isobar-analogue concept, the potential for the $^2S_{1/2}$ wave of the n^{12}C scattering with parameters obtained for the p^{12}C scattering

$$V_S = 102.05 \text{ MeV}, \ \alpha_S = 0.195 \text{ fm}^{-2}, \quad (11)$$

which do not lead to the resonance as it is shown by dash curve in Fig. 1a if Coulomb potential is switch off was tried. It gives the total radiative capture cross sections several orders less comparing the experimental data within the treated energy range from 25 meV up to 1 MeV.

Let us turn to the potential describing well ^2S-phase shift with parameters from[49]

$$V_S = 98.57558 \text{ MeV}, \ \alpha_S = 0.2 \text{ fm}^{-2}. \quad (12)$$

Phase shift of this potential is given by solid line in Fig. 1a, and dash curve in Fig. 1b shows corresponding WF. The parameters of potential (12) are given with high accuracy for correct description of binding energy in the $^2S_{1/2}$ wave laying at -1.856907 MeV towards the threshold of the n^{12}C channel. Note, if we switch off the Coulomb interaction in initial $^2S_{1/2}$ potential, determined for the p^{12}C scattering for correct reproducing of the above-threshold resonance at 0.42 MeV, this state becomes bound. So, the potential in the n^{12}C channel, besides the forbidden, has one allowed bound state corresponding to the first excited state (ES) of ^{13}C at 3.089 MeV with $J^\pi = 1/2^+$ towards its GS.

Total cross section obtained with (2) for BS and scattering potential (12) is shown by dashed curve in Fig. 2a. Calculated cross section is twice as lower than experimental data at 25 meV[18], and it lies a little lower than data[21] and[22] in the energy range 20-200 KeV. For comparison, let us consider results with the same scattering potential (12), but with GS potential (10), which describes AC correctly. They are shown in Fig. 2a by dotted line. It is seen that they lead to correct description of total cross sections obtained in different experimental investigations, beginning from the energy 25 meV to 550 KeV. The calculation results for transition from the $^2D_{3/2}$ scattering wave with potential (12) at $L = 2$ and coefficient in cross section for $J_i = 3/2$ for GS of ^{13}C with potential of (10) are shown by dot-dashed line. The scattering phase shift of the D wave is within 1 at the energy less than 1 MeV. The solid line is the sum of dotted and dot-dashed lines, i.e., the sum of transitions $^2S_{1/2} \to {}^2P_{1/2}$ and $^2D_{3/2} \to {}^2P_{1/2}$.

We would like to emphasize that these results have been obtained for the potentials (12) and (10) conformed GS characteristics of ^{13}C, viz. with the asymptotic constant and low energy n^{12}C elastic scattering phase shifts. Thereby, this combination of potentials, describing the characteristics of both discrete and continuous spectra of the n^{12}C system, allows to reproduce well available experimental data on the radiative neutron capture cross sections for transitions to the GS in the energy range from 25 meV up to 550 KeV covering seven orders. Now treating transitions on to exciting states we want to remark that AC given in[54] for the first ES $1/2^+$ of ^{13}C in the n^{12}C channel is equal to 1.61 fm$^{-1/2}$, and recalculated with $\sqrt{2k} = 0.76$ to dimensionless value turned to be 2.12. Besides, in[13-16] the AC equals 1.84(16) fm$^{-1/2}$ was obtained for the first ES, or its recalculated value is 2.42(17).

In the present case the $E1$ transition from the $P_{1/2}$ and $P_{3/2}$ scattering waves onto the $S_{1/2}$ binding excited state in the n^{12}C channel (12) is assumed. As the P wave has no FS, and there are no negative parity resonances in spectrum of ^{13}C then corresponding potentials may be regarded zero. While constructing a potential for the binding ES we would orient on the reproducing of the mentioned AC value, as its width affects weakly on the mean square radius.

As a result, the potential (12) with FS was used for excited BS in the $S_{1/2}$ wave. It leads to the binding energy of -1.856907 MeV with accuracy 10^{-6} by FDM, charge radius of 2.48 fm, mass radius of 2.67 fm, and AC equals 2.11(1) within the interval of 6-24 fm. AC values do not differ too much from results of[13-16]. Total cross sections given in Fig. 2b by solid line display reasonable agreement with experimental data at low energies.

Asymptotic constant for the second excited state $3/2^-$ of ^{13}C calculated in[54] is 0.23 fm$^{-1/2}$, or 0.33 after recalculation to the dimensionless value with $\sqrt{2k} = 0.69$. For getting the appropriate value of the AC, the potential must be very narrow:

$$V_{3/2} = 681.80814 \text{ MeV}, \ \alpha_{3/2} = 2.5 \text{ fm}^{-2}. \quad (13)$$

This potential gives the binding energy of -1.261840 MeV with accuracy of 10^{-6} by FDM, charge radius of 2.47 fm, mass radius of 2.44 fm, and the AC equals 0.30(1) within the interval of 2-24 fm. It does not have FS, and reproduces the AC rather well[54].

The calculated cross sections of the neutron capture on ^{12}C from the $^2S_{1/2}$ scattering state with potential (12) to the $^2P_{3/2}$ level are given in figure 2c by dotted line together with experimental data[18, 21-24]. Dashed line shows the calculation results for the cross section with transition to this ES from the $^2D_{3/2}$ and $^2D_{5/2}$ scattering waves for potential (12) at $L = 2$ and exact coefficients in cross sections for $J_i = 3/2$ and 5/2. Solid line shows the sum of these cross sections. It is well seen that developing approach allows us to obtain acceptable results in description of total cross sections at the transition to the second ES of ^{13}C. Thereby, the intercluster potentials are conformed to scattering phase shifts as usual and, in the large, correctly describe the main characteristics of the considered BS, which is the second ES of ^{13}C.

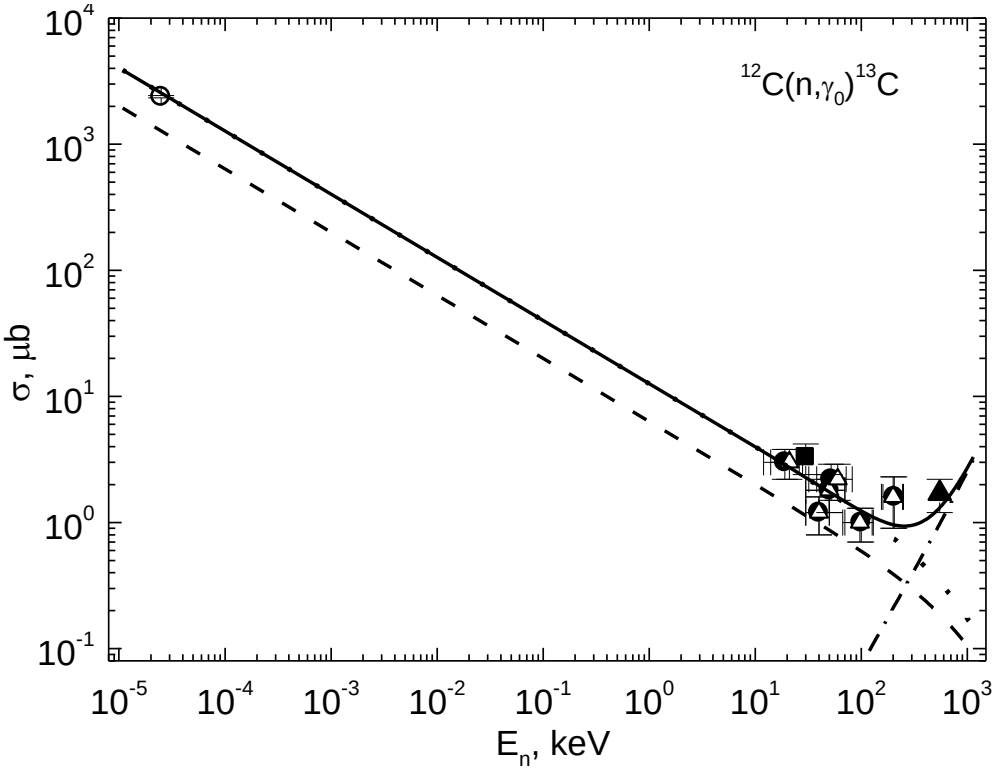

Figure 2a. The total cross sections of the radiative neutron capture on ^{12}C on the ground state of ^{13}C at low energies. Experimental data: black squares (■) –[22], black dots (●) –[23] and[24], open triangles (Δ) –[21], open circles (○) –[18] and closed triangles (▲) –[19]. Solid line – total cross section calculated with GS potential (8) and scattering potential (12); dash curve – with GS (10) and scattering state (12)

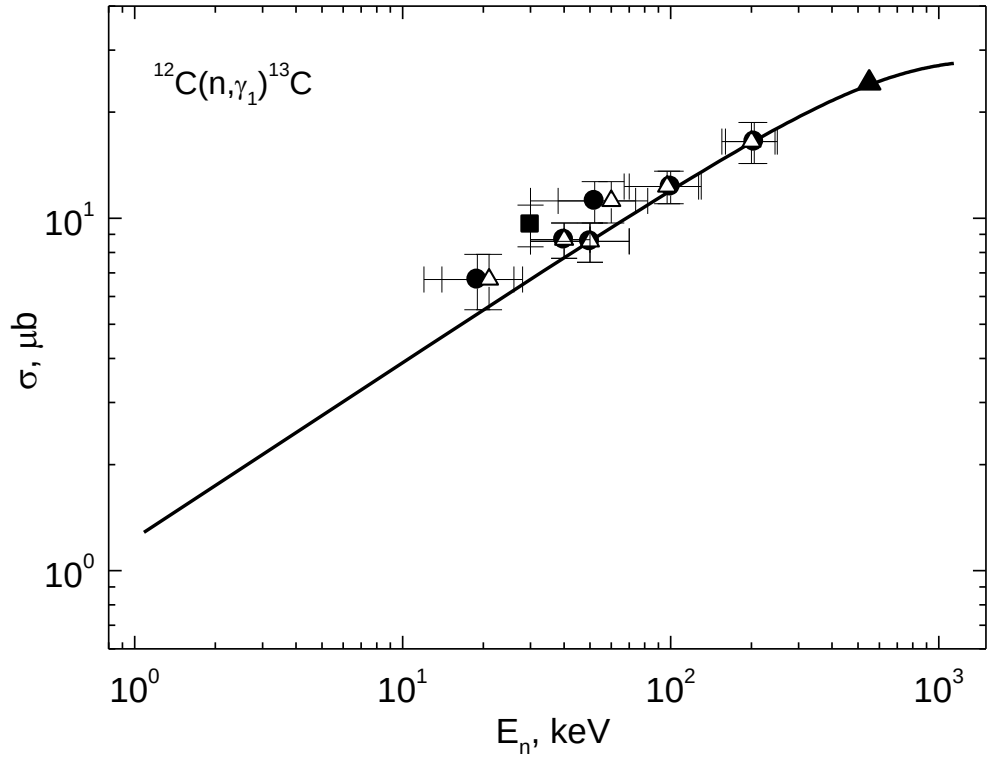

Figure 2b. The total cross sections of the radiative neutron capture on ^{12}C on the first excited state $1/2^+$ of ^{13}C at low energies. Experimental data: black squares (■) –[22], black dots (●) –[23] and[24], open triangles (Δ) –[21], closed triangles (▲) –[19]. Solid line – total cross section calculated with ES potential (12) and scattering *P* potential with zero depth

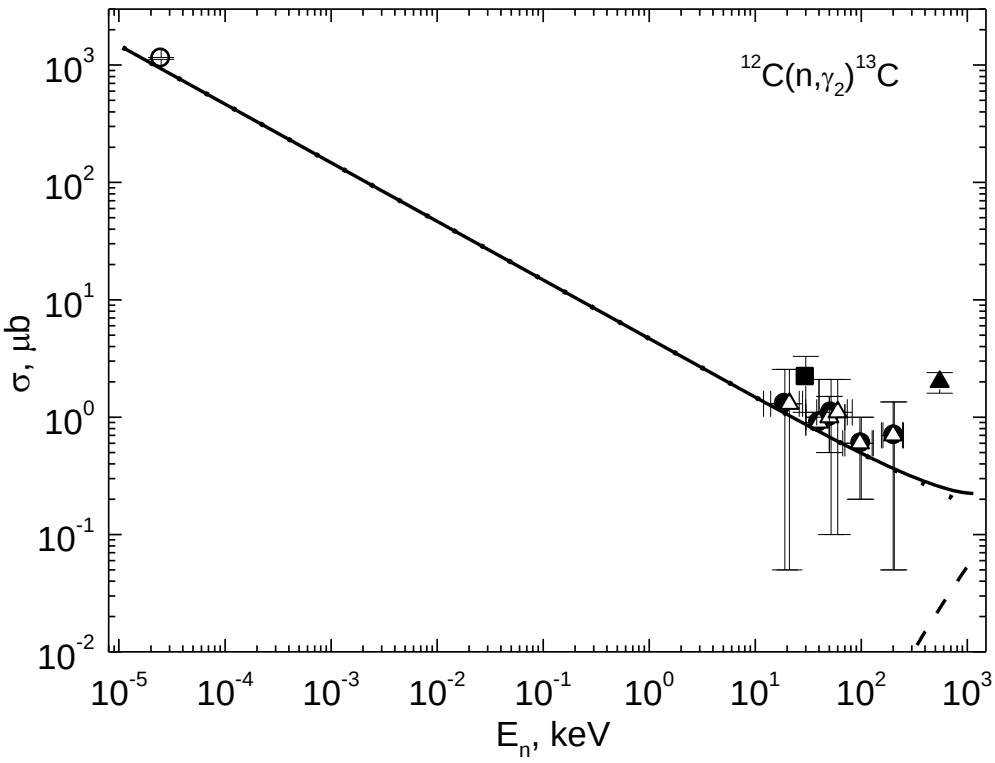

Figure 2c. The total cross sections of the radiative neutron capture on ^{12}C on the second excited state $3/2^-$ of ^{13}C at low energies. Experimental data: black squares (■) –[22], black dots (●) –[23] and[24], open triangles (Δ) –[21], open circles (○) –[18] and closed triangles (▲) –[19]. Solid line – total cross section calculated with ES potential (12) and scattering $P_{3/2}$ potential (13)

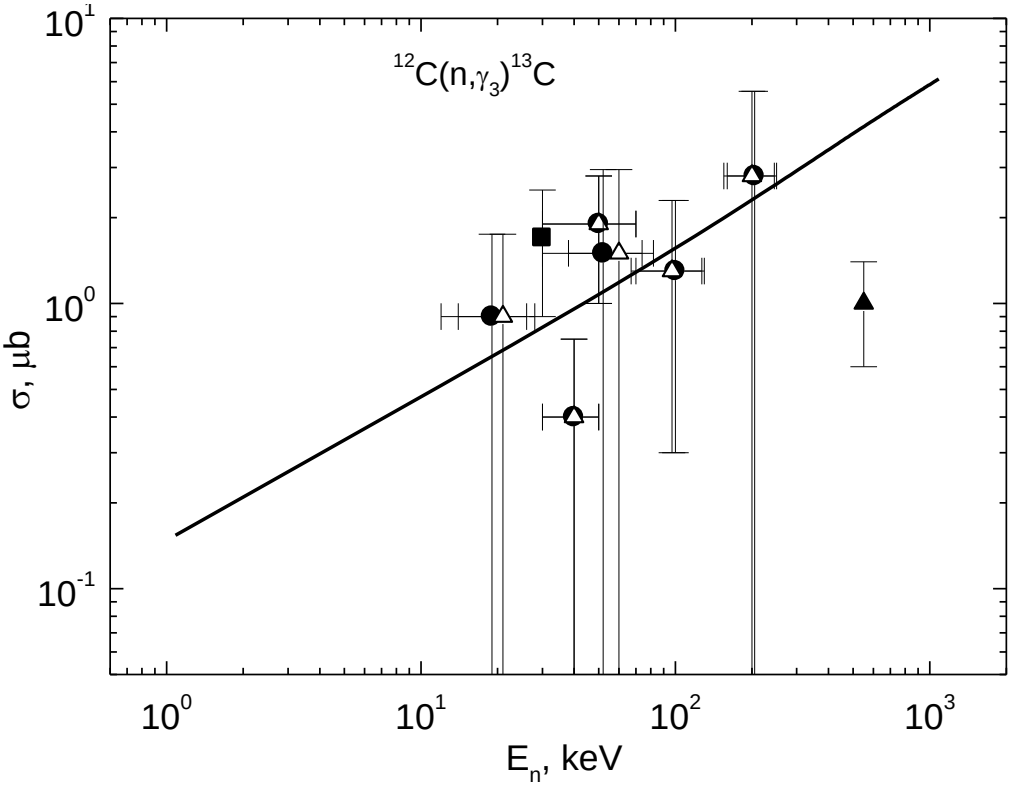

Figure 2d. The total cross sections of the radiative neutron capture on ^{12}C on the third excited state $5/2^+$ of ^{13}C at low energies. Experimental data: black squares (■) –[22], black dots (●) –[23] and[24], open triangles (Δ) –[21], closed triangles (▲) –[19]. Solid line – total cross section calculated with ES potential (14) and scattering *P* potential with zero depth

Let us present the AC for consideration of the transitions from $P_{3/2}$ scattering wave onto binding $D_{5/2}$ state at the energy of -1.09254 MeV relatively the threshold of $n^{12}C$ channel, which is the third excited state in ^{13}C. The value of 0.11 $fm^{-1/2}$ was obtained in[54], and in[13-16] it is 0.15(1) $fm^{-1/2}$. Recalculated values at $\sqrt{2k} = 0.665$ turn to be 0.16 and 0.23. Zero potential for the $P_{3/2}$ scattering wave was used as before. For the binding $D_{5/2}$ state a potential (10) with one FS and same geometry as for the GS of ^{13}C was used

$$V_D = 263.174386 \text{ MeV}, \alpha_D = 0.2 \text{ fm}^{-2}. \quad (14)$$

It gives the binding energy of -1.092540 MeV with accuracy of 10^{-6} by FDM, the charge radius of 2.49 fm, the mass radius of 2.61 fm, and the AC equals 0.25(1) within the interval of 6-25 fm. It has FS, and reproduces properly the order of magnitude of the AC.

The calculated cross sections of the radiative neutron capture on ^{12}C from the $^2P_{3/2}$ scattering state onto the binding $^2D_{5/2}$ level are shown in Fig. 2d by the solid line together with experimental data. Thus, in this case too, the PCM allows us to obtain quite reasonable results in description of total cross sections for the capture to the third ES of ^{13}C. In addition, the intercluster potentials are agreed with scattering phase shifts as usual and correctly reproduce the main characteristics of each considered BS in the $n^{12}C$ channel.

As at the energies from 10^{-5} to 10 KeV the calculated cross section σ_{theor} is practically straight line (solid line in Fig. 2a) it may be approximated at low energies by simple function

$$\sigma_{ap} = \frac{A}{\sqrt{E_n}}. \quad (15)$$

Constant value A = 12.7292 μb $(KeV)^{1/2}$ is defined by one point of cross sections at the minimal energy 10^{-5} KeV. Modulus of relative deviation between the calculated σ_{theor} and approximated σ_{ap} cross sections

$$M(E) = \left|[\sigma_{ap}(E) - \sigma_{theor}(E)]/\sigma_{theor}(E)\right| \quad (16)$$

in the energy range from 10^{-5} up to 10 KeV is less than 1.0%. We would like to assume the same energy dependence shape of the total cross section at lower energies. So, implemented estimation of cross section done at 1 μeV according (15) resulted 402.5 mb.

4. Total Cross Sections for Neutron Capture on ^{13}C

Total cross sections for the radiative capture $n^{13}C \rightarrow {}^{14}C\gamma$ process have been calculated with the potential of Gaussian form (2) with zero Coulomb term. As the $^3S_1$ wave potential without FS we used firstly the parameters fixed for the $p^{13}C$ scattering channel[28]

$$V_S = 265.4 \text{ MeV}, \alpha_S = 3.0 \text{ fm}^{-2}. \quad (17)$$

Fig. 3 shows the result of the $^3S_1$ phase shift calculation (dashed curve) with the $p^{13}C$ potential without Coulomb interaction, but for the scattering $n^{13}C$-channel. It does not reveal now the resonance behavior[29], but depends smoothly from energy. As there is no FS in this system this phase shift starts from zero value.

Potential with one FS of triplet bound $^3P_0$ state should reproduce properly the binding energy of ^{14}C in $J^\pi = 0^+$ ground state equals in the $n^{13}C$-channel -8.1765 MeV (see work[32]) as well as describe the mean square radius of ^{14}C according the experimental value 2.4962(19) fm[32]. The appropriate parameters have been obtained basing on the start set for ^{14}N in the bound $p^{13}C$ state

$$V_{GS} = 399.713125 \text{ MeV}, \alpha_{GS} = 0.45 \text{ fm}^{-2}. \quad (18)$$

This potential gives the binding energy of -8.176500 MeV with FDM accuracy of 10^{-6} and the charge mean square radius R_{ch} = 2.47 fm and the mass radius of 2.47 fm. For the asymptotic constant in dimensionless form[37, 38] value of 1.85(1) was obtained in the interval of 4-12 fm being averaged by pointed above interval. Note, that the value of 1.81(26) $fm^{-1/2}$ was obtained for the AC in this channel[55], and after the recalculation at $\sqrt{2k} = 1.102$ its dimensionless value 1.65(24) is in agreement with the present calculations.

As the additional computing control for the calculation of binding energy variational method was applied[36]. It gave the energy value of -8.176498 MeV with dimension N = 10 and independent parameter varying of potential (18). Charge radius and asymptotic constant do not differ from those obtained by FDM. It should be marked that the averaged value for the true binding energy in the discussed potential might be regarded the average value of -8.176499(1) MeV obtained by FDM and VM procedures within the computing accuracy of ±1.0 eV.

We like to comment that experimental data on the total cross sections of the radiative neutron capture on ^{13}C given in Fig. 4 are taken from[18, 23, 24, 56-60] and were obtained from the Moscow State University data base[25]. Fig. 4 shows the pointed experimental data for the energies 25 meV-100 KeV.

For the description of total cross sections as in[28] we accounted the $E1$ transition from the non-resonating scattering $^3S_1$ and $^3D_1$ waves obtained with central potential (13) to the bound triplet $^3P_0$ state of ^{14}C with $J^\pi = 0^+$ in the $n^{13}C$ channel generated by potential (18). Calculated total cross sections for $^{13}C(n, \gamma_0)^{14}C$ process at the energies lower 1.0 MeV with defined potential sets overestimate by near two orders the experimental data[23, 24, 56] in the region 10-100 KeV.

Experimental data from[58-60] at 25 meV may be reproduced if take the potential depth

$$V_S = 215.77045 \text{ MeV}, \alpha_S = 3.0 \text{ fm}^{-2}. \quad (19)$$

for the $^3S_1$ wave at the same geometry. The corresponding phase shift and total cross section are given by solid curves in Figs. 3 and 4, respectively. The scattering potential describes properly the bound $^3S_1$ level with $J^\pi = 1^-$ in the $n^{13}C$ channel but excited at 6.0938 MeV, and leads to the binding energy of -2.08270 MeV relatively the threshold, charge and mass radii of 2.47 fm, and the AC equals 1.13(1) within the

interval of 2-22 fm. The situation here is similar to those in previous system when the above-threshold resonance $^3S_1$ state in the p^{13}C system becomes bound one if the Coulomb interaction is switch off.

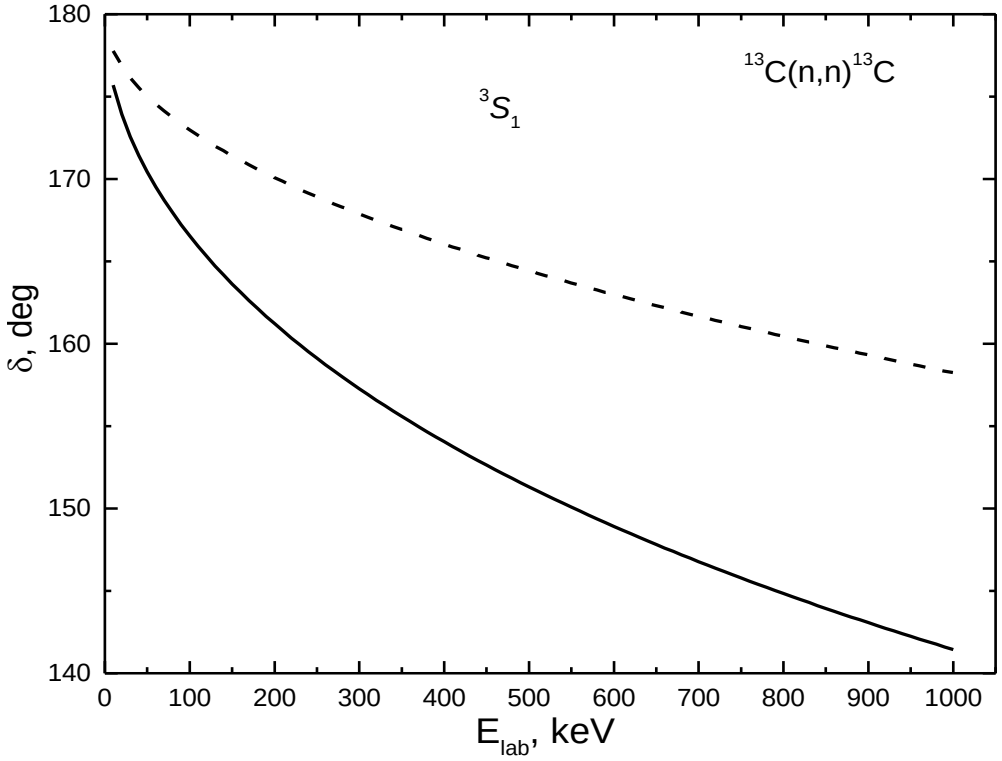

Figure 3. Low energy $^3S_1$ phase shift of the n^{13}C elastic scattering. Dash curve – calculations with potential (17): solid – modified (19)

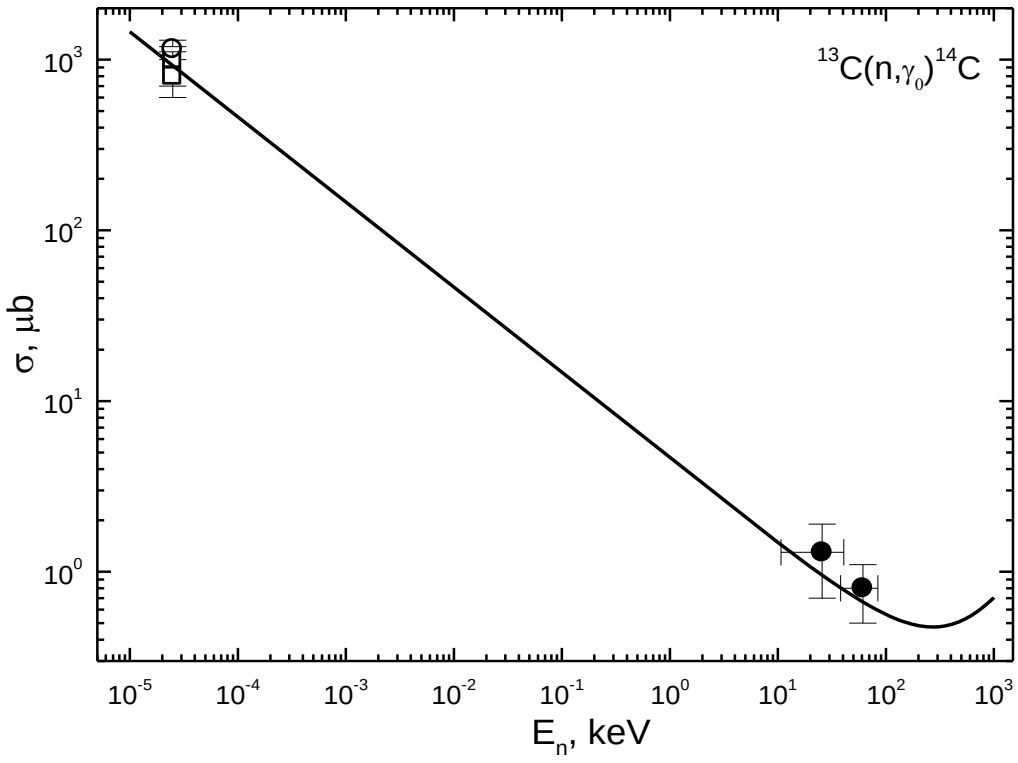

Figure 4. The total cross sections of the radiative neutron capture on ^{13}C on the ground state of ^{14}C at low energies. Experimental data: black dots (•) –[23] and[24], open squares (□) –[57-60], open circles (○) –[18]. Calculations with GS potential (18) and modified scattering potential (19)

Consequently it is seen that slight change of potential depth coordinated with the energy of the $^3S_1$ binding level allows to reproduce the experimental data on the total capture cross sections from 25 meV up to 100 KeV (see Fig. 4). Slowdown of the cross section at 0.5-1.0 MeV is coming due to the $E1$ transition from the $^3D_1$ scattering wave which input is noticeable in this energy region only. Estimation of the $M2$ transition from the resonating $^3P_2$ scattering wave corresponding to the $J^\pi = 2^+$ at 141 KeV in c.m. to the $^3P_0$ ground state shows near 1% input from the $E1$ cross section.

Specially should be mentioned that comparing the previous n^{12}C system we did not find any independent information on AC for the first ES in binding $^3S_1$ wave. That is why scattering potential (19) may have some ambiguity in parameters. We do not exclude that there might be another set of parameters which may describe correctly the characteristics of bound state, in particular binding energy and total capture cross sections, but leading to somewhat another asymptotic constant.

The evaluation of cross section value of the $M2$ transition from the resonance $J^\pi = 2^+$ at 152.9(1.4) KeV (l.s.) $^3P_2$ scattering wave with very small width 3.4(0.7) KeV (c.m.) (see work[32]) to the $^3P_0$ GS leads to the value that is less than 1% from the cross section of the $E1$ process. However, it is possible to find the $E1$ transition from the $^3P_2$ resonance scattering wave to the $^3S_1$ first ES of ^{14}C with energy of 6.0938 MeV at $J = 1^-$ with the obtained potential (19). The cross section of this process is to have narrow resonance, which can reach the value of 1–2 mb. At first, for carrying out of these calculations, we will find the potential of the $^3P_2$ resonance wave without FS, which has parameters:

$$V_P = 10719.336 \text{ MeV}, \alpha_P = 40.0 \text{ fm}^{-2}. \quad (20)$$

This potential leads to the resonance energy of 153 KeV (l.s.) with the width of 3.7 KeV (c.m.), and its phase shift is shown in Fig. 5 by the solid line. The next parameters were found for the potential of the $^3P_2$ resonance wave that has bound FS:

$$V_P = 46634.035 \text{ MeV}, \alpha_P = 60.0 \text{ fm}^{-2}. \quad (21)$$

It leads to the resonance at 153 KeV with the width of 4.0 KeV, the scattering phase shift with this potential is shown in Fig. 5 by the dashed line. This potential is coordinated with the given above classification according to Young tableaux, supposing that the AS in this partial wave is not bound.

In both cases, the phase shift of the potentials at resonance energy has the value 90.0(5) degrees, and widths of the potentials are in a good agreement with the experimental data and are in the range of their errors at 3.4(0.7) KeV, the same as the resonance energies at 152.9(1.4) KeV[32]. Here, the parameters of the potentials are obtained fully unambiguously in both cases if the number of FS is given, though they have rather exotic values. The depth of the potential identifies the location of the resonance, and its width gives the calculated width of this resonance.

Let us present now the calculation results of the $E1$ transition with these two potentials. In the first case, for potentials (19) and (20), the results are shown by the dotted line in Fig. 6. The dashed line shows results for total cross sections with the transition to the GS, shown in Fig. 4 by the solid line. The solid line in Fig. 6 is the sum of these cross sections. The experimental data for summarized cross sections with the transitions to the GS and all ES are given in[23, 24, 61-63] and are shown in Fig. 6 by black squares and open triangles at 30 KeV[61] and 40 KeV[62]. The summarized cross sections at resonance energy have the values of 1.42 mb, which can be used for comparison, if the new measurements of total capture cross section in the resonance region will be done.

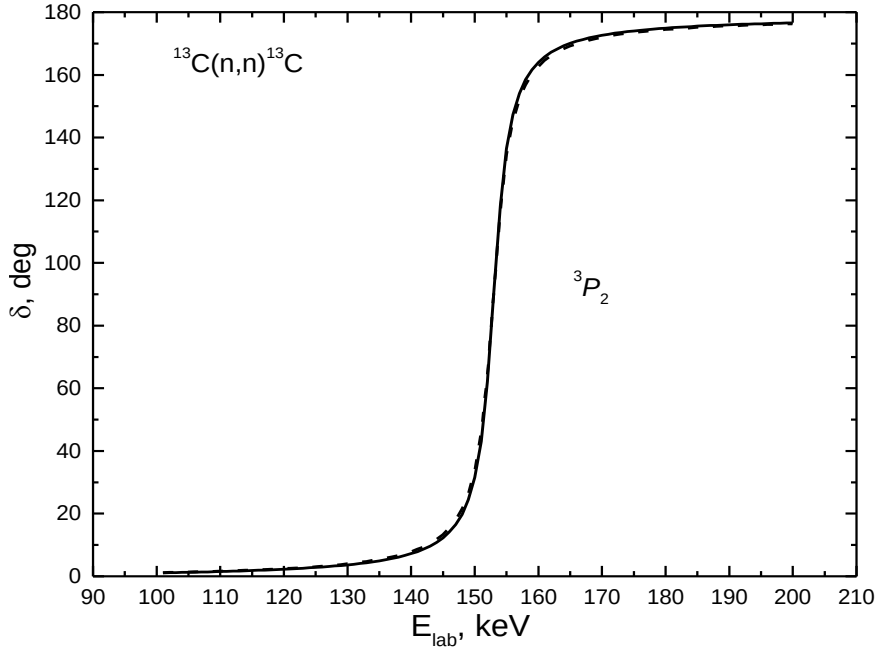

Figure 5. The $^3P_2$ phase shift of the n^{13}C elastic scattering at low energies. Lines – the solid line is for potential without FS and with width of resonance at 3.7 KeV and the dashed line is for potential with one bound FS and with width of resonance at 4.0 KeV

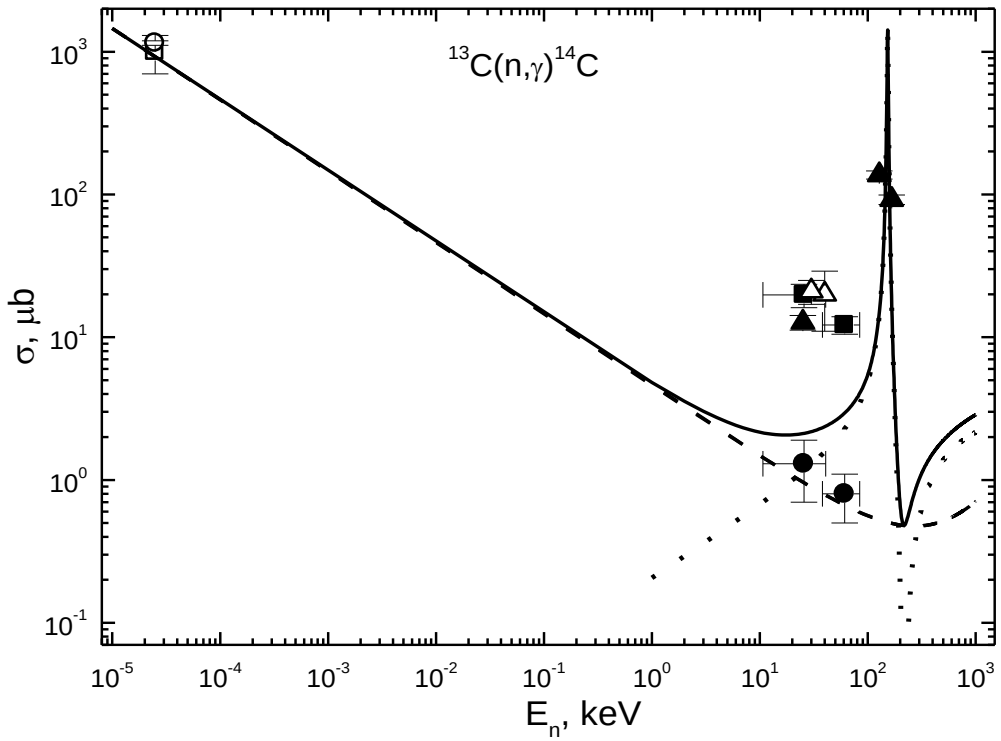

Figure 6. The total cross section of the radiative neutron capture on ^{13}C for transitions to the GS and to the first ES of ^{14}C. Experimental data: • –[23] and[24], □ –[58-60], ○ –[18] – for transitions to the GS and Δ – at 30 KeV from work[61], at 40 KeV from[62], ■ –[23],[24] and ▲ –[63] for total summarized capture cross sections. Lines: dashed – the calculation of total cross sections for transitions to the GS, dotted – transition to the first ES and solid – summed cross section

Let us note that the results of work[63], shown in Fig. 6 by triangles, came to light for us after carrying out all calculations of the total cross sections and, as seen from the figure, they have wonderful agreement with the resonance part of cross sections.

The analogous calculation results for scattering potential (21) practically do not differ from the given in Fig. 6. Only, the summarized cross sections at the resonance energy have the slightly smaller value, which is equal to 1.40 mb, this can be caused by the certain increasing of the width of the resonance for potential containing the bound FS (21). Thus, the results of both calculations practically do not depend from the presence of the bound FS in the $^3P_2$ resonance potential. They are absolutely determined by the correctness of reproduction of the resonance energy level and, in the first place, its width.

Furthermore, we did not succeed in search of the n^{13}C phase shift analysis and experimental data on elastic scattering differential cross sections at the energies below 1.0 MeV. The available data above 1.26 MeV[64] were measured with too large energy step and are not appropriate for the phase shift analysis contrary to the procedure applied successfully for the p^{12}C, n^{12}C and p^{13}C systems at energies below 1.0 MeV[30, 49]. Let us note that for the p^{13}C scattering in the resonance region at 0.55 MeV and its width of 23(1) KeV there were near 30 measurements of differential cross sections, done by several groups at four scattering angles. So, detailed data allowed us to correctly reproduce the shape of resonance at $J^\pi T = 1^-1$ and 8.06 MeV relatively to the GS of ^{14}N or 0.551(1) MeV relatively to the threshold of the p^{13}C channel[32] within the phase shift analysis[29].

In this case, the differential cross sections of the n^{13}C elastic scattering data of[62] available above 1.26 MeV are given with too large energy step and they are not appropriate for reproducing the shape of the resonance with $J^\pi = 1^-$ at 9.8 MeV relatively to the GS or at 1.75 MeV (l.s.) relatively to the n^{13}C threshold. Parameters of this resonance are given in Table 14.7[32]. The situation with information on the $^3P_2$ wave of the n^{13}C elastic scattering which may correspond to $J^\pi = 2^+$ resonance at 153 KeV (l.s.) with width of 3.4 KeV (c.m.) is even worse. Therefore, there is no possibility to obtain the $^3P_2$ and $^3S_1$ scattering phase shifts from the experimental data on differential cross sections at low energies and to construct potentials on their basis. However, the usage of some other criteria for construct of the intercluster potentials allows us to find their parameters, which leads to the appropriate description of the available experimental data.

Thus, the BS interaction of the n^{13}C system reproduces characteristics of the GS of ^{14}C quite well, as it was obtained previously for the p^{13}C channel of ^{14}N[28]. However, the absence of the results on the AC leads to the impossibility to do certain and final conclusions about parameters of the potential (19) in the $^3S_1$ wave. In other respects, the situation is analogous to the previous one from the n^{12}C system, when changes of the *S* phase shift for scattering process did not limited by the Coulomb interaction only. The real *S* phase

shift of the $n^{12}C$ scattering, obtained in the phase shift analysis has slightly small values than the calculated phase shift of the $p^{12}C$ potential with switched off Coulomb interaction[65].

Since in the energy interval from 10 meV up to 10 KeV the calculated cross section is practically straight line it may be approximated by simple function like (15) with constant of A = 4.6003 μb $(KeV)^{1/2}$. It was defined by one point of cross section at minimal energy equals 10 meV obtained with parameters set (17) for elastic scattering $^3S_1$ potential and shown in Fig. 4. Modulus of relative deviation between the calculated σ_{theor} and approximated σ_{ap} cross sections defined above as $M(E)$ in the energy range from 25 meV up to 10 KeV is less than 0.4%. We would like still to assume the same energy dependence shape of the total cross section at lower energies. So, estimation of cross section that was done at 1 μeV according (15) gives 145.5 mb.

5. Conclusions

Present results show that appropriate $n^{12}C$ scattering potential (12) coordinated with corresponding phase shifts [49] together with correct reproducing of ^{13}C GS enable to describe the available experimental data on the radiative neutron capture cross sections at the energies from 25 meV to 100 KeV. All potentials satisfied the classification of FS and AS by orbital Young tableaux. Potential constructed for the GS reproduces the basic characteristics of ^{13}C, i.e., binding energy in the $n^{12}C$ channel, mean square radius and asymptotic constant.

Constructed within the PCM two-body $n^{13}C$ potentials for the $^3S_1$ wave and ^{14}C GS, show good results for the total neutron radiative capture on ^{13}C in the energy range from 25 meV up to 100 KeV. Two-body potential used for the bound $n^{13}C$-system reproduces well the basic GS characteristics of ^{14}C, as well as it was done for ^{14}N in the $p^{13}C$ channel[28]. Our results for the radiative neutron capture on ^{13}C for transitions to the GS and to the first ES of ^{14}C are in a wonderful agreement with the experiment data[63], which became known for us after finishing these calculations.

So, these results may be regarded as one more confirmation of the success of cluster model approach applied earlier to the radiative neutron processes in other twenty systems[66], including succeeded also in description of radiative capture reactions of protons and other charge clusters on light nuclei[1-3].

ACKNOWLEDGMENTS

This work was supported by the Grant Program No. 0151/GF2 of the Ministry of Education and Science of the Republic of Kazakhstan "The study of thermonuclear processes in the primordial nucleosynthesis of the Universe".

We would like to express our thanks to Professor R. Yarmukhamedov for the detailed consultations on the asymptotic normalization constants for the treated channels.

REFERENCES

[1] S. B. Dubovichenko, Thermonuclear Processes of the Universe (NOVA Sci. Publ., New-York, 2012).https://www.novapublishers.com/catalog/product_info.php?products_id=31125.

[2] S. B. Dubovichenko, Yu. N. Uzikov, Phys. Part. Nucl. 42, 251 (2011).

[3] S. B. Dubovichenko and A. V. Dzhazairov-Kakhramanov, Astrophysical S-Factors of Proton Radiative Capture in Thermonuclear Reactions in the Stars and the Universe, in: The Big Bang: Theory, Assumptions and Problems ed. by Jason R. O'Connell and Alice L. Hale (NOVA Publishers, New York, 2012), 1-60.; https://www.novapublishers.com/catalog/product_info.php?products_id=21109.

[4] C. A. Barnes, D. D. Clayton and D. N. Schramm, Essays in Nuclear Astrophysics Presented to William A. Fowler (Cambridge University Press, Cambridge, 1982).

[5] J. A. Peacock Cosmological Physics (Cambridge University Press, Cambridge, 1999).

[6] V. G. Neudatchin, V. I. Kukulin, V. N. Pomerantsev and A. A. Sakharuk, Phys. Rev. C 45, 1512 (1992).

[7] S. B. Dubovichenko, Phys. Atom. Nucl. 58, 1174 (1995).

[8] S. B. Dubovichenko, Phys. Atom. Nucl. 61, 162 (1998).

[9] O. F. Nemets, V. G. Neudatchin, A. T. Rudchik, Yu. F. Smirnov and Yu. M. Tchuvil'sky, Nucleon Association in Atomic Nuclei and the Nuclear Reactions of the Many Nucleons Transfers (Naukova dumka, Kiev, 1988).

[10] E. G. Adelberger et al., Rev. Mod. Phys. 83, 195 (2011).

[11] V. I. Kukulin, V. G. Neudatchin, I. T. Obukhovsky and Yu. F. Smirnov, Clusters as subsystems in light nuclei, in: Clustering Phenomena in Nuclei, Vol. 3, edited by K. Wildermuth and P. Kramer (Vieweg, Braunschweig, 1983) 1.

[12] S. B. Dubovichenko, J. of Exp. and Theor. Phys. 113, 221 (2011).

[13] M. Heil et al., Astrophys. J. 507, 997 (1998).

[14] V. Guimaraes and C. A. Bertulani, AIP Conf. Proc. 1245, 30 (2010); available online at: arXiv:0912.0221v1[nucl-th] 1 Dec 2009.

[15] M. Igashira and T. Ohsaki, Sci. Tech. Adv. Materials 5, 567 (2004); available online at: http://iopscience.iop.org/1468-6996/5/5-6/A06.

[16] Y. Nagai et al., Hyperfine Interactions 103, 43 (1996).

[17] Z. H. Liu et al., Phys. Rev. C 64, 034312 (2001).

[18] S. F. Mughabghab, M. A. Lone and B. C. Robertson, Phys. Rev. C 26, 2698 (1982).

[19] T. Kikuchi et al., Phys. Rev. C 57, 2724 (1998).

[20] R. L. Macklin, Astrophys. J. 357, 649 (1990).

[21] T. Ohsaki et al., Astrophys. J. 422, 912 (1994).

[22] Y. Nagai et al., Nucl. Instr. Meth. B 56/57, 492 (1991).

[23] T. Shima et al., JAERI-C-97-004, 131 (1996).

[24] T. Shima et al., Nucl. Phys. A 621, 231 (1997).

[25] http://cdfe.sinp.msu.ru/exfor/index.php.

[26] http://www-nds.iaea.org/exfor/exfor.htm.

[27] S. B. Dubovichenko and A. V. Dzhazairov-Kakhramanov, Rus. Phys. J. 52, 833 (2009).

[28] S. B. Dubovichenko, Phys. Atom. Nucl. 75, 173 (2012).

[29] S. B. Dubovichenko, Phys. Atom. Nucl. 75, 285 (2012).

[30] S. B. Dubovichenko, Rus. Phys. J. 51, 1136 (2008).

[31] V. G. Neudatchin and Yu. F. Smirnov, Nucleon associations in light nuclei (Nauka, Moscow, 1969).

[32] F. Ajzenberg-Selove, Nucl. Phys. A 523, 1 (1991).

[33] C. Itzykson and M. Nauenberg, Rev. Mod. Phys. 38, 95 (1966).

[34] S. B. Dubovichenko and A. V. Dzhazairov-Kakhramanov, Euro. Phys. Jour. A 39, 139 (2009).

[35] S. B. Dubovichenko, Rus. Phys. J. 54, 157 (2011).

[36] V. I. Kukulin et al., Nucl. Phys. A 517, 221 (1990).

[37] G. R. Plattner et al., Phys. Lett. B 61, 21 (1976).

[38] N. Lim, Phys. Rev. C 14, 1243 (1976).

[39] C. Angulo et al., Nucl. Phys. A 656, 3 (1999).

[40] S. B. Dubovichenko and A. V. Dzhazairov-Kakhramanov, Phys. Part. Nucl. 28, 1615 (1997).

[41] http://xxx.lanl.gov/abs/1201.1741

[42] http://physics.nist.gov/cgi-bin/cuu/Category?view=html&Atomic+and+nuclear.x=78&Atomic+and+nuclear.y=12

[43] http://cdfe.sinp.msu.ru/services/ground/NuclChart_release.html

[44] A. Mengoni, T. Otsuka and M. Ishigara, Phys. Rev. C 52, R2334 (1995).

[45] C. J. Lin et al., Phys. Rev. C 68, 047601 (2003).

[46] A. Likar and T. Vidmar, Nucl. Phys. A 619, 49 (1997).

[47] H. Kitazawa and K. Go, Phys. Rev. C 57, 202 (1998).

[48] D. Baye, Phys. Rev. C 70, 015801 (2004).

[49] S. B. Dubovichenko, Rus. Phys. J. 55, 561 (2012).

[50] R. O. Lane et al., Ann. der Phys. 12, 135 (1961).

[51] F. Ajzenberg-Selove, Nucl. Phys. A 506, 1 (1990).

[52] A. M. Mukhamedzhanov and N. K. Timofeyuk, J. Sov. Nucl. Phys. 51, 431 (1990).

[53] L. D. Blokhintsev, A. M. Mukhamedzhanov and N. K. Timofeyuk, Ukrainian J Phys. 35, 341 (1990).

[54] J. T. Huang, C. A. Bertulani and V. Guimaraes, Atom. Data and Nucl. Data Tabl. 96, 824 (2010).

[55] E. I. Dolinskii, A. M. Mukhamedzhanov, R. Yarmukhamedov, Direct nuclear reactions on light nuclei with the emission of neutrons (FAN, Tashkent, 1978).

[56] A. Wallner et al., J. Phys. G 35, 014018 (2008).

[57] B. J. Allen and R. L. Macklin, Phys. Rev. C 3, 1737 (1971).

[58] G. A. Bartholomew, Atomic Energy of Canada Limited (AECL) 1472, 39 (1961).

[59] G. A. Bartholomew et al., Atomic Energy of Canada Limited (AECL) 517, 30 (1957).

[60] G. R. Hennig, Phys. Rev. 95, 92 (1954).

[61] Z. Y. Bao et al., Atom. And Nucl. Data Tabl. 76, 70 (2000).

[62] S. Raman, M. Igashira, Y. Dozono et al., Phys. Rev. C 41, 458 (1990).

[63] A. Wallner et al., Publications of the Astronomical Society of Australia (PASA) 29, 115 (2012).

[64] R. O. Lane et al., Phys. Rev. C 23, 1883 (1981).

[65] S. B. Dubovichenko, Phys. Atom. Nucl. 76, 894 (2013).

[66] S. B. Dubovichenko, A. V. Dzhazairov-Kakhramanov, Ann. der Phys. 524, 850 (2012).